

^{18}O states via the $^{14}\text{C}(^6\text{Li},d)^{18}\text{O}$ reaction at 34 MeV incident energy

A. Cunsolo, A. Foti, G. Immè, G. Pappalardo, and G. Raciti

Istituto Nazionale di Fisica Nucleare, Sezione di Catania, Centro Siciliano di Fisica Nucleare e di Struttura della Materia, Istituto di Fisica dell'Università di Catania, Corso Italia 57, 95129 Catania, Italy

N. Saunier

Département de Physique Nucléaire Centre d'Etude Nucléaire de Saclay, Boîte Postale 2, 91190, Gif sur Yvette, France

(Received 25 November 1980)

The reaction $^{14}\text{C}(^6\text{Li},d)^{18}\text{O}$ is studied at 34 MeV ^6Li incident energy in the $5^\circ \leq \theta_{\text{lab}} \leq 45^\circ$ angular range in steps of 5° . Angular distributions are analyzed in terms of Hauser-Feshbach and exact finite range distorted-wave Born-approximation theories. The direct α -transfer cross sections are evaluated in both the hypotheses of transfer to pure and mixed configurations. In the mixed configurations case good agreement between experimental and theoretical cross sections is found by using the empirical wave functions of Lawson, Serduke, and Fortune. Alpha-spectroscopic strengths are extracted for ^{18}O states lying below 17.0 MeV excitation energy. Spins and parities are suggested for the 7.84, 8.9, 12.04, 14.6, and 17.0 MeV ^{18}O levels. The existence and the structure of a positive-parity ^{18}O rotational band is investigated.

NUCLEAR REACTIONS $^{14}\text{C}(^6\text{Li}, d)^{18}\text{O}$ $E=34$ MeV; measured $\sigma(\theta)$; ^{18}O levels deduced J^π and S_α . HF and EFR-DWBA analysis. EFR-DWBA analysis using empirical wave functions.

I. INTRODUCTION

In the last few years the structure of the ^{18}O nuclear states has been the subject of many theoretical works.¹⁻¹¹ As pointed out by these works, the simple shell-model description of ^{18}O as two neutrons outside an inert ^{16}O core is inadequate even at low excitation energy, and admixtures with m -particle n -hole core excitation must be taken into account. In particular, the wave functions of the positive parity ^{18}O states lying below 7.2 MeV excitation energy, have been described by Lawson *et al.*⁴ as a linear combination of two particles in (sd) shell and collective deformed $4p$ - $2h$ states, with (sd)⁴(p)⁻² components. The wave function mixing amplitudes were empirically determined by fitting single-nucleon¹² and two neutrons (t, p) transfers,¹³ as well as static and dynamic electromagnetic data.

In a similar analysis, done by Erikson and Brown,⁹ the deformed states to admix with $2p$ configurations were constructed by introducing a highly deformed intrinsic state. The mixing amplitudes were calculated best fitting the ^{18}O spectrum by assuming a rotational band, based on the 0^+ level at 3.63 MeV, similar to that of the ^{20}Ne ground state.

Buck *et al.*^{5,10} have shown that, in the framework of a folding potential model, some positive and negative parity ^{18}O states are well accounted for by four and trinucleon cluster states, respectively. In particular, these authors have proposed that the 2_3^+ at 5.26 MeV, the 4_2^+ at 7.11 MeV, and

the 6_1^+ at 11.69 MeV ^{18}O states, described as $\alpha + ^{14}\text{C}$ cluster states, are excellent candidates for rotational states built on the 0_2^+ level at 3.63 MeV. On the other hand, in a recent investigation done by Rudra¹⁴ within the framework of a collective Hamiltonian including rotation-vibration coupling, two bands were proposed: the first based on the g.s. 0_1^+ level (the 2_1^+ at 1.98 MeV and the 4_1^+ at 3.55 MeV being the other members) and the second one on the 0_2^+ at 3.63 MeV (the other members being the 2_2^+ at 3.92 MeV and the 4_2^+ at 7.11 MeV). Sakuda *et al.*^{7,8} have shown that the known α -transfer data,¹⁵ the $E2$ transitions, and the energies of both the known positive and negative parity ^{18}O states are well described by mixing $2p$ or $3p$ - $1h$ shell model states with α clustering of $4p$ - $2h$ states.

From the experimental point of view, in order to check α -cluster components of nuclear wave functions α -transfer reactions are expected to be a very powerful tool. Up to now, only the $^{14}\text{C}(^7\text{Li}, t)^{18}\text{O}$ at 20.4 MeV incident energy has been reported by Morgan *et al.*¹⁵ By using the ^{18}O wave functions of Lawson *et al.*⁴ and the ($^7\text{Li}, t$) data of Morgan *et al.*,¹⁵ Fortune and Kurath¹¹ have successfully analyzed in the exact-finite-range-distorted-wave Born-approximation (EFR-DWBA) framework the transitions to the ^{18}O positive parity states lying below 7.2 MeV excitation energy. In order to provide new information it seemed worthwhile to investigate the $^{14}\text{C}(^6\text{Li}, d)^{18}\text{O}$ reaction at 34 MeV incident energy. At this energy the ($^6\text{Li}, d$) reaction should be dominated by a dir-

ect α transfer to the target nucleus.¹⁶

Preliminary results have been reported elsewhere.¹⁷ Section II deals with the experimental procedure. An empirical separation procedure, applied to some unresolved doublets, is presented in Sec. III. Section IV is devoted to the analysis of data in terms of statistical compound nucleus and EFR-DWBA formalisms. The direct cross section is calculated in both the hypothesis of α transfer to pure and mixed 2p and 4p-2h configurations. Relative α -spectroscopic strengths are analyzed in detail for low-lying ^{18}O positive parity states and some evidence of an ^{18}O positive-rotational band is presented. In Sec. V conclusions about the ^{18}O states discussed in the present work are summarized.

II. EXPERIMENTAL PROCEDURE AND RESULTS

The measurements were performed at the Centre d'Etude Nucléaire de Saclay using a 34 MeV $^6\text{Li}^{3+}$ beam produced by the FN-Tandem Van de Graaff. The beam intensity, measured at the Faraday cup was typically about 100 nA.

In order to obtain cross sections in absolute values, we measured the elastic scattering of a 34 MeV ^6Li beam on a $150 \pm 10 \mu\text{g}/\text{cm}^2$ Au target at forward angles, where Rutherford law holds. The emitted particles were detected in the angular range $5^\circ \leq \theta_{\text{lab}} \leq 45^\circ$ in steps of $\Delta\theta = 5^\circ$ using a cooled ΔE - E counter telescope. The ΔE was a

surface barrier silicon detector 200 μm thick, the E was a silicon detector 5000 μm thick. Particle identification was performed by processing the E and ΔE signals in a standard way.¹⁷ Each event was processed by a 620 L Varian computer, for on-line control of the experiment and, at the same time, stored on magnetic tape for off-line analysis. A silicon detector 200 μm thick, was fixed at 30° for monitoring both the relative values and the natural carbon buildup on the target.

Self-supporting ^{14}C targets enriched to 70% and $45 \pm 9 \mu\text{g}/\text{cm}^2$ thick were obtained by a cracking procedure,¹⁸ evaporating CH_3I on a heated Ni foil and chemically dissolving the Ni backing. The total ($^{12}\text{C} + ^{14}\text{C}$) target thickness was deduced by measuring the straggling and energy loss in the target of α particles emitted from a standard radioactive source and detected by means of the Saclay quadrupole-dipole-dipole-dipole (QDDD) magnetic spectrometer. The ^{14}C percentage was obtained from target beta activity measurements. An uncertainty of 20% on absolute cross sections is assumed, mainly due to target thickness nonuniformity. A typical deuteron spectrum is shown in Fig. 1. The energy calibration was obtained from known transitions in ^{18}O and ^{16}O . The overall energy resolution [full width at half maximum (FWHM)] was about 75 keV.

All the identified deuteron groups are labeled in Fig. 1 according to the excitation energy of the

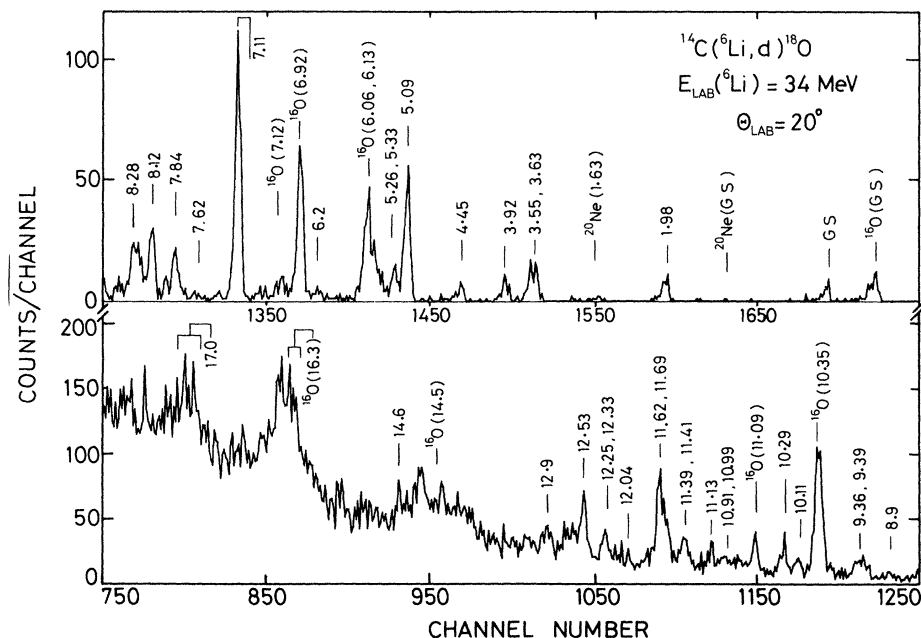


FIG. 1. Deuteron energy spectrum from the $^{14}\text{C}(^6\text{Li}, d)^{18}\text{O}$ reaction at $E(^6\text{Li}) = 34$ MeV.

levels populated in ^{18}O . The main features of this spectrum are as follows:

(i) All the known¹ positive-parity ^{18}O levels are populated. In particular, the candidates for rotational states built on the first excited 0^+ at 3.63 MeV [i.e., the 3.92 MeV(2^+), proposed in Ref. 14; the 7.11 MeV(4^+) (Refs. 5 and 14), and the 12.53 MeV(6^+) (Ref. 15)] are strongly populated. In addition the g.s. (0^+), the 1.98 MeV(2^+), and the 3.55 MeV(4^+) levels, described^{4,7,9} as “two-particles” main configuration, and the 10.29 MeV(4^+) level are clearly seen.

(ii) The negative-parity states at 4.45 MeV(1^-), 5.09 MeV(3^-), and 8.12 MeV(5^-) excitation energy are strongly populated.

(iii) The level at 7.84 MeV, that probably does not correspond to the 2^+ at 7.8 MeV with a 6p-4h configuration observed in the $^{12}\text{C}(^{18}\text{O}, ^{12}\text{C})^{18}\text{O}$ reaction,¹⁹ is excited likewise in the $(^7\text{Li}, t)$ reaction,¹⁵ but not as strongly as in the $^{15}\text{N}(^6\text{Li}, ^3\text{He})^{18}\text{O}$ reaction.²⁰ In Ref. 20, a $J^\pi = 5^-$ spin and parity value was proposed by assuming a 3p-1h main structure for this state. On the other hand, by assuming a mixing of 2p-0h and collective configurations, with a slight dominance (~60%) of the first, Sakuda suggested in Ref. 7 a $J^\pi = 4^+$ assignment. Both of these predictions are not inconsistent with the above experimental findings.

(iv) The 11.13 and 14.6 MeV states probably correspond to the 11.10 and 14.61 MeV ones seen more strongly in the $(^6\text{Li}, ^3\text{He})$ reaction.²⁰ For

both of these levels, $J^\pi = 6^-$ or 7^- spin and parity values were proposed in Ref. 20.

(v) The 12.04 MeV level, weakly excited in the α -elastic scattering,²¹ is clearly populated.

(vi) Above the tail of a continuous deuteron spectrum, interpreted¹⁶ as due to the ^6Li breakup, a broad peak (FWHM ~300 keV) is observed in the 17 MeV excitation energy region. This peak cannot contain the known¹ 17.02 MeV ($T=2$) level, since the $^{14}\text{C}(^6\text{Li}, d)$ reaction selects only ^{18}O $T=1$ states. In the following we shall assume that this peak is due to excitation of only one state.

Unfortunately some interesting doublets are unresolved. However the [3.55 MeV(4^+) + 3.63 MeV(0^+)], the [5.26 MeV(2^+) + 5.33 MeV(0^+)], and the [11.39 MeV(2^+) + 11.41 MeV(4^+)] doublets may be analyzed with a procedure explained in Sec. III. Their angular distributions are shown in Fig. 2. The [11.62 MeV(5^-) + 11.69 MeV(6^+)] and [12.25 MeV(1^-) + 12.33 MeV(5^-)] doublets are analyzed in Sec. IV. For the doublets (9.36 MeV + 9.39 MeV) and (10.91 MeV + 10.99 MeV) of unknown spins and parities only the experimental cross sections are reported. The deuteron angular distributions for all the observed transitions are shown in Figs. 3–6. The angular distribution shape is typical of a given l transfer. This finding qualitatively confirms that, at our incident energy, the reaction proceeds predominantly via a direct α -transfer mechanism.

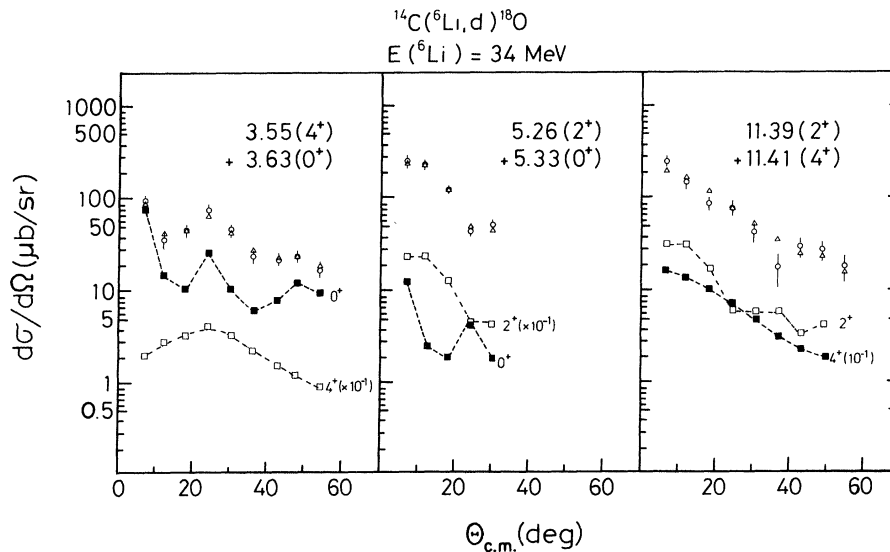


FIG. 2. Angular distribution of deuterons leading to the doublets at $|3.55 \text{ MeV} + 3.63 \text{ MeV}|$, $|5.26 \text{ MeV} + 5.33 \text{ MeV}|$, and $|11.39 \text{ MeV} + 11.41 \text{ MeV}|$ reported as open circles. Solid and open squares refer to the single A_i $(d\sigma/d\Omega)_i$ components; triangles refer to the sum $(d\sigma/d\Omega)_{\text{WD}} = A_1(d\sigma/d\Omega)_1 + A_2(d\sigma/d\Omega)_2$ (see text). Dashed curves are drawn to guide the eyes.

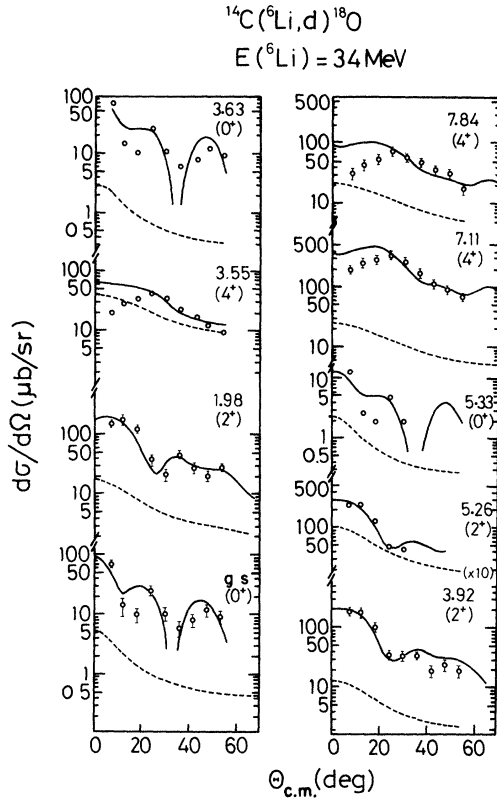


FIG. 3. Angular distribution of deuterons from the $^{14}\text{C}(^6\text{Li},d)^{18}\text{O}$ reaction at $E(^6\text{Li})=34$ MeV leading to positive parity ^{18}O states. The dashed curves represent HF calculations, the full ones represent the incoherent sum of HF and EFR-DWBA contributions.

III. EMPIRICAL DOUBLETS RESOLUTION

By neglecting interference effects, the experimental whole doublet cross section (WD) can be expressed as

$$\left(\frac{d\sigma}{d\Omega}\right)_{\text{WD}} = A_1 \left(\frac{d\sigma}{d\Omega}\right)_{s_1} + A_2 \left(\frac{d\sigma}{d\Omega}\right)_{s_2}, \quad (1)$$

$(d\sigma/d\Omega)_{s_i}$ being the shape of the cross section of the i th member and A_i the relative weight factor.

If the $(d\sigma/d\Omega)_{s_i}$ shapes are known, the A_i factors can be extracted via a fitting procedure of the data based on a linear two parameters least square method. Two different choices can be made for these shapes. The first one based on theoretical reaction mechanism predictions (see Sec. IV B), and the second on "empirical" information. In the following we discuss the empirical procedure.

If the i th member of a doublet and a nearby level both have the same spin and parity, and if both

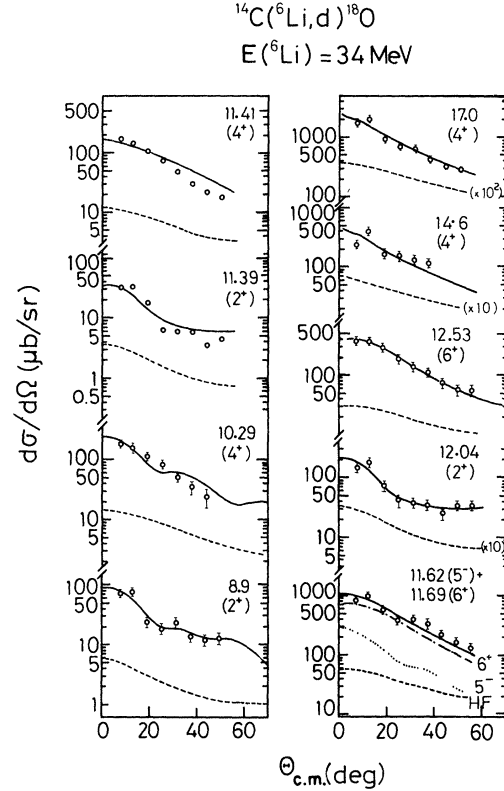


FIG. 4. Same as Fig. 3. The two dashed curves labeled as 5^- and 6^+ represent the incoherent sum of HF and EFR-DWBA theoretical calculations for the 11.62 MeV (5^-) and 11.69 MeV (6^+) transitions, respectively. In this case the full curve is the sum of these two components. The dashed curve labeled as HF is also the sum of the two HF contributions.

are populated through the *same* mechanism, their angular distribution shapes are expected to be very similar. If these hypotheses hold, $(d\sigma/d\Omega)_{\text{WD}}$ can be reproduced consistently, replacing in Eq. (1) the $(d\sigma/d\Omega)_{s_i}$ shape with the experimentally known angular distribution of a transition to a "similar" level. This procedure was applied to the doublets of known spin and parity components; the A_i values and the χ^2 values obtained are reported in Table I. These χ^2 values are compared in Table I with those obtained when the reaction mechanism predictions (see Sec. IV B) were used. For each doublet the A_i values with the best χ^2 value were selected.

In particular the "empirical" procedure was preferred for the [3.55 MeV(4^+) + 3.63 MeV(0^+)], [5.26 MeV(2^+) + 5.33 MeV(0^+)], and [11.39 MeV(2^+) + 11.41 MeV(4^+)] doublets. This procedure was also checked both by comparing with the few experimental values obtained when the doublets were resolved, as well as by reproducing the whole

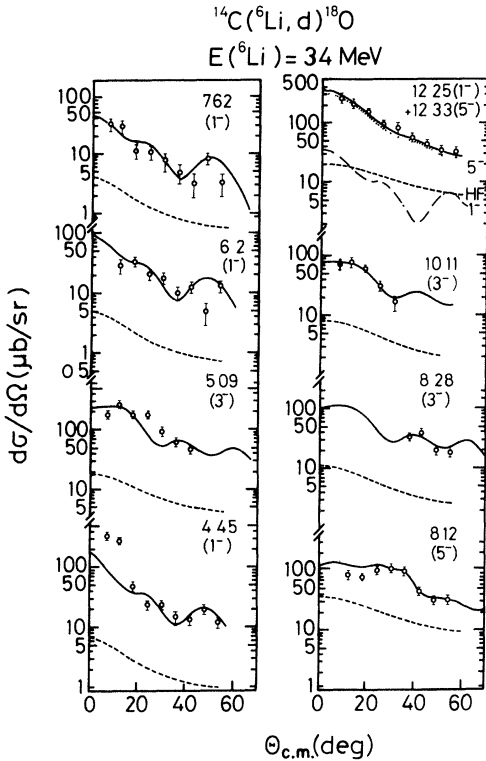


FIG. 5. Same as Fig. 3 but for transitions leading to negative parity ^{18}O states. The full and dashed curves for the doublet at $|12.25 \text{ MeV}(1^-) + 12.33 \text{ MeV}(5^-)|$ have the same meaning as for the doublet at $|11.62 \text{ MeV}(5^-) + 11.69 \text{ MeV}(6^+)|$ in Fig. 4.

TABLE I. Results of the doublet analysis (see text).

Doublet	Similar levels	A_i	χ_{EDR}^{2a}	$\chi_{\text{th.pr}}^{2a}$
3.55(4 ⁺)	7.11(4 ⁺)	0.20	0.36	3.73
3.63(0 ⁺)	g.s. (0 ⁺)	1.02		
5.26(2 ⁺)	3.92(2 ⁺)	1.33	0.29	0.88
5.33(0 ⁺)	g.s. (0 ⁺)	0.19		
11.39(2 ⁺)	3.92(2 ⁺)	0.17	1.90	3.33
11.41(4 ⁺)	10.29(4 ⁺)	0.90		
11.62(5 ⁻)	8.12(5 ⁻)	0.28	3.00	1.93
11.69(6 ⁺)	12.53(6 ⁺)	2.21		
12.25(1 ⁻)	7.62(1 ⁻)	6.18	3.55	0.47
12.33(5 ⁻)	8.12(5 ⁻)	0.38		

^aThe χ^2 values were evaluated by $\chi^2 = (1/N) \sum_{i=1}^N [(\sigma_{\text{WB}}^{\text{exp}} - \sigma_{\text{WB}}^{\text{calc}})^2 / \Delta\sigma_{\text{WB}}^{\text{exp}}]$. χ_{EDR}^{2a} refers to "empirical" procedure. $\chi_{\text{th.pr}}^{2a}$ refers to theoretical predictions (EFR-DWBA and HF) procedure.

doublet's angular distributions. This last check is shown in Fig. 2 where the triangles are the re-constructed values [see Eq. (1)] and the solid and open squares are the evaluated $A_i(d\sigma/d\Omega)_{s_i}$ single components. As shown in Fig. 2 good consistency was achieved. In the following we shall treat these $A_i(d\sigma/d\Omega)_{s_i}$ values, empirically obtained, as data.

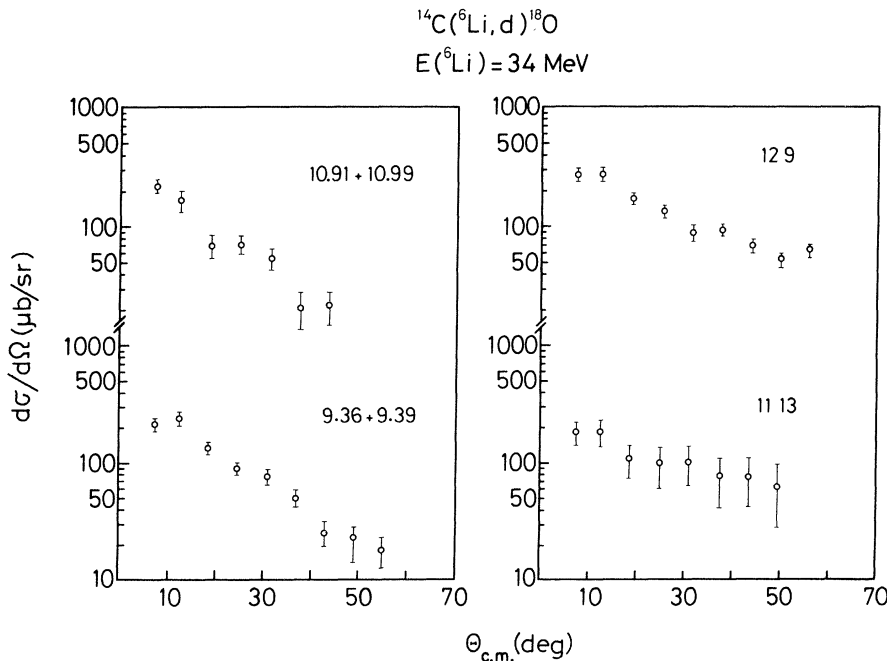


FIG. 6. Angular distribution of deuterons leading to unknown spin and parity ^{18}O states.

TABLE II. Optical model parameters used in HF calculations. For the spin-orbit potential we have used the same radius and diffuseness as in the real part. The radii dependence is $R = r A^{1/3}$.

Channel	V^a (MeV)	r_V (fm)	a_V (fm)	W (MeV)	r_W (fm)	a_W (fm)	r_C (fm)	V_{so}^b (MeV)	Δ (MeV)	Ref.
$^6\text{Li} + ^{14}\text{C}$	250.0	1.354	0.65	30.0 ^b	1.354	0.65	2.0		5.2	28,30
$n + ^{19}\text{F}$	c	1.309	0.66	b,e	1.260	0.48	1.309		2.7	38
$p + ^{19}\text{O}$	d	1.25	0.65	8.005 ^b	1.250	0.47	1.250	7.5	2.35	39
$d + ^{18}\text{O}$	92.92	1.044	0.814	10.1 ^b	1.395	0.709	1.3		5.05	40
$t + ^{17}\text{O}$	146.8	1.400	0.55	19.3 ^a	1.400	0.55	1.3		2.35	41
$\alpha + ^{16}\text{N}$	200.0	1.26	0.63	5.0 ^a	1.600	0.60	1.25		0.	42

^aForm factor: Woods-Saxon.

^bForm factor: Woods-Saxon derivative W_D .

^cEnergy dependence: $V(E) = 47.01 - 0.267 E - 0.00118 E^2$.

^dEnergy dependence: $V(E) = 58.762 - 0.55 E$.

^eEnergy dependence: $W(E) = 9.52 - 0.53 E$.

IV. ANALYSIS OF THE DATA AND RESULTS

In order to analyze our data we have described the $(^6\text{Li}, d)$ reaction in terms of incoherent contributions²² coming from the direct α transfer, evaluated in the EFR-DWBA framework, and from the statistical compound nucleus reaction mechanism, evaluated following the Hauser-Feshbach (HF) formalism.²³

A. Hauser-Feshbach calculations

Hauser-Feshbach (HF) calculations have been carried out in the same formalism as that of Ref. 22. The optical model parameters used are reported in Table II. In order to check the absolute value of the calculated HF cross sections we have normalized to the structureless angular distribution of the 5.22 MeV level of ^{17}O weakly populated in the $^{14}\text{C}(^6\text{Li}, t)^{17}\text{O}$ at $E(^6\text{Li}) = 34$ MeV (Ref. 17) by assuming a $(\frac{3}{2}^-)$ spin and parity.²⁴ The obtained HF normalization factor was further tested by reproducing the direct one-step forbidden transition to the 2.31 MeV $0^+ ^{14}\text{N}$ level observed in the $^{14}\text{C}(^6\text{Li}, ^6\text{He})^{14}\text{N}$ reaction at the same incident energy.²⁵ The normalized HF theoretical curves,

drawn as dashed lines in Figs. 3–5, account only for $\sim 10\%$ the experimental cross sections.

B. EFR-DWBA calculations: “pure configurations”

The direct cross section has been evaluated in the EFR-DWBA formalism using the SATURN-MARS I code of Tamura and Low,²⁶ assuming a single-step α transfer, without spin flip, from ^6Li to the ^{14}C . The ^6Li was described as α - d clusters in a relative $2S$ state. The α - ^{14}C relative motion wave functions were generated in a Woods-Saxon well whose depth was adjusted to reproduce the known α -separation energies. The other parameters are reported in Table III. The number of nodes N and the orbital angular momentum L were fixed by the Talmi-Moshinsky relationship

$$2N + L = \sum_{i=1}^4 (2n_i + l_i), \quad (2)$$

where n_i and l_i are the harmonic oscillator quantum numbers of each transferred nucleon. It is implicitly assumed in Eq. (2) that the four nucleons correlate to form a cluster with zero quanta of internal excitation.

Since elastic scattering data were not available,

TABLE III. Optical-model parameters used in EFR-DWBA calculations.

Channel	V^a (MeV)	r_V (fm)	a_V (fm)	W^b (MeV)	r_W (fm)	a_W (fm)	r_C (fm)	Ref.
$^6\text{Li} + ^{14}\text{C}$	250.0	1.354 ^c	0.650	30.0	1.354 ^c	0.650	2.0 ^c	28,30
$d + ^{18}\text{O}$	92.92	1.044 ^c	0.814	10.1	1.395 ^c	0.709	1.3 ^c	40
$^{14}\text{C} + \alpha$	d	1.250 ^c	0.650				1.25 ^c	22
$d + \alpha$	d	1.545 ^c	0.650				1.545 ^c	28

^aForm factor: Woods-Saxon.

^bForm factor: Woods-Saxon derivative W_D .

^c $R = rA^{1/3}$.

^dVaried to reproduce separation energies.

^e $R = r(A^{1/3} + a^{1/3})$.

TABLE IV. α -spectroscopic strengths for positive-parity ^{18}O levels by assuming α transfer to pure-configuration two-particles (S_6) or 4p-2h (S_8).

Ex (MeV)	J_i^π	$S_6 \times 10^{2^a}$	$S_8 \times 10^{2^a}$	Ex (MeV)	J_i^π	$S_6 \times 10^{2^a}$	$S_8 \times 10^{2^a}$
0.0	0_1^+	4.4	2.6	11.69	6_1^+	3.2	3.3
1.98	2_1^+	11.4	1.2	12.04	2_6^+	7.7	3.9
3.55	4_1^+	3.2	0.16	12.53	6_2^+	2.4	1.51
3.63	0_2^+	5.5	3.6	14.6	4_6^+	4.5	4.2
3.92	2_2^+	14.8	1.6	17.0	4_7^+	31.1	24.4
5.26	2_3^+	24.1	2.8				
5.33	0_3^+	1.2	0.79				
7.11	4_7^+	10.6	4.0				
7.84	4_3^+	2.7	1.2				
8.9	2_4^+	2.7	1.4				
10.29	4_4^+	3.1	2.1				
11.39	2_5^+	1.3	0.61				
11.41	4_5^+	2.5	1.8				

^aEstimated absolute uncertainties $\pm 25\%$ [statistical errors ($\sim \pm 10\%$), absolute values uncertainty ($\sim \pm 20\%$)].

many sets of optical-model parameters for entrance and exit channels were tested to reproduce the shape of our data. The best agreement was found by using the optical-model parameters (OMP) listed in Table III. We remark that these OMP are essentially the *same* optical-model parameters employed successfully in our previous analysis of the $^{12}\text{C}(^6\text{Li}, d)^{16}\text{O}$ reaction done at the same incident energy²² and that, in a systematic way, account for $(^6\text{Li}, d)$ reactions in nuclei of (sd) and (fp) shells.²⁷⁻³¹ Levels above 6.23 MeV excitation energy in ^{18}O are unbound against α -particle emission; for these levels the separation-energy extrapolation method^{22,32} was used. By comparing the incoherent sum of the EFR-DWBA and the HF calculations with experimental angular distributions we extracted the spectroscopic strengths S defined as

$$\frac{d\sigma}{d\Omega} = S \left(\frac{d\sigma}{d\Omega} \right)_{\text{EFR-DWBA}} + \left(\frac{d\sigma}{d\Omega} \right)_{\text{HF}} \quad (3)$$

Table IV summarizes the S values obtained by assuming α transfer to 2p or to 4p-2h pure components for each ^{18}O positive parity level, labeled S_6 and S_8 , respectively (where the subscripts denote the numbers of quanta in $\alpha + ^{14}\text{C}$ radial wave functions).

In Table V the reported S_7 values were obtained for the negative-parity ^{18}O levels by assuming α transfer to 3p-1h components. Note that, as mentioned in Sec. III, the spectroscopic strengths S_i for the members of the [11.62 MeV(5^-) + 11.69 MeV(6^+)] and [12.25 MeV(1^-) + 12.33 MeV(5^-)] doublets were extracted, via a least square method,

using the relationship

$$\left(\frac{d\sigma}{d\Omega} \right)_{\text{WD}} = S_1 \left(\frac{d\sigma}{d\Omega} \right)_{\text{EFR-DWBA}}^{(1)} + \left(\frac{d\sigma}{d\Omega} \right)_{\text{HF}}^{(1)} + S_2 \left(\frac{d\sigma}{d\Omega} \right)_{\text{EFR-DWBA}}^{(2)} + \left(\frac{d\sigma}{d\Omega} \right)_{\text{HF}}^{(2)}. \quad (4)$$

The theoretical and experimental angular distributions are compared in Figs. 3–5. In general good agreement was found. The present results are consistent with previously¹ known spins and parities of the ^{18}O states up to 12.5 MeV excitation energy. The angular distribution shape of the 7.84 MeV level deviates in the forward angular range from an $l=4$ DWBA curve in the same way as the one for the known 4^+ state at 7.11 does.

TABLE V. α -spectroscopic strengths for negative-parity ^{18}O levels, by assuming α transfer to 3p-1h pure configuration.

Ex (MeV)	J_i^π	$S_7 \times 10^{2^a}$
4.45	1_1^-	2.3
5.09	3_1^-	2.3
6.2	1_2^-	2.3
7.62	1_3^-	1.2
8.12	5_1^-	1.6
8.28	3_2^-	1.9
10.11	3_3^-	1.58
11.62	5_2^-	(1.4 \pm 2.2)
12.25	1_4^-	(1.1 \pm 2.4)
12.33	5_3^-	1.3

^aAs in Table IV.

This fact suggests an empirical 4^+ assignment, in agreement with the Sakuda theoretical prediction.⁷ The 8.9 MeV level data agree with an $l=2$ curve, suggesting a 2^+ tentative assignment. A 2^+ assignment is also suggested for the 12.04 MeV level, corroborating the indication given by Morgan *et al.*²¹ from an α -elastic scattering analysis. The 11.13 and 12.9 MeV data agree with more than one curve, so we cannot draw any suggestion about their spins. However, HF calculations done assuming $J^\pi=6^+$, as suggested in Ref. 20, for both the 11.13 and 14.6 MeV states, give cross sections about six and eleven times, respectively, smaller than the experimental ones. Furthermore for the 14.6 MeV data, the best agreement was obtained with an $l=4$ DWBA curve.

At higher excitation energy we have analyzed the angular distribution of the peak at 17.0 MeV. The experimental shape seems to agree with an $l=4$ DWBA curve. In addition, preliminary d - α angular correlation measurements¹⁷ seem to confirm this $J^\pi=4^+$ assignment.

C. "Mixed configurations" analysis

As proposed in Refs. 11 and 33 the configuration mixing in the wave functions of the residual nuclear states can be tested through a DWBA analysis. In this case, the direct cross section cannot be factorized into a spectroscopic strength factor S and a DWBA cross section as in Eq. (3), but becomes³⁴

$$\left(\frac{d\sigma}{d\Omega}\right)_{\text{DWBA}}^{\text{MC}} = \left| \alpha_{2s} \sum_{NL} A_{NL} B_{NL,2s}(\theta) \right|^2. \quad (5)$$

The $B_{NL,2s}(\theta)$ is the usual transition amplitude. The A_{NL} is the product of the α_{NL} spectroscopic amplitude for the ^{18}O nucleus in a definite state,

dissociating into an $\alpha + ^{14}\text{C}_{\text{g.s.}}$ system with relative motion specified by N and L quantum numbers, times the C_{NL} weight coefficient of the (NL) configuration in the wave function. The α_{2s} term is simply the spectroscopic amplitude for the ^6Li nucleus dissociating into an $\alpha + d$ system with $N=2, L=0$ relative motion. This is considered constant for all the transitions.

Following Fortune and Kurath,¹¹ taking the collective component of the low-lying ^{18}O states wave functions to be $4p-2h$ with $(sd)^4$ particles being a ^{20}Ne and the $(1p)^{-2}$ holes being the $^{14}\text{C}_{\text{g.s.}}$, the A_{NL}^J terms for α transfer to a state of spin J are

$$A_{NL}^J = C_{NL}^J \left(\frac{18}{14}\right)^4 \left(\frac{3}{128}\right) \sqrt{70}. \quad (6)$$

On the other hand, the A_{NL}^J for α transfer to $2p$ components are

$$A_{NL}^J = \left(\frac{18}{14}\right)^3 \left(\frac{3}{32}\right) \sqrt{30} \sum_{J_1 \geq J_2} C_{NL}^{J_1 J_2} \langle \text{amp for } \nu(J_1 J_2) \Pi(1p)^2 0 \rangle, \quad (7)$$

where

$$C_{NL}^{J_1 J_2} = C_{NL}^{J_1} D(J_1, J_2, J),$$

and the $D(J_1, J_2, J)$ coefficients are the weight factors for shell-model neutron configurations. The A_{NL}^J values for the ^{18}O positive parity states below 7.2 MeV excitation energy were calculated by Fortune and Kurath¹¹ by using the C_{NL}^J and $C_{NL}^{J_1 J_2}$ coefficients obtained by Lawson *et al.*⁴ Table VI summarizes the A_{NL}^J , listed as A_6 and A_8 .

For the transition amplitudes $B_{NL,2s}(\theta)$ calculations, optical model and bound-state parameters were taken to be exactly the *same* as in Sec. IV B. In order to perform the coherent sum over (NL) in Eq. (5), we used a modified version of the **SATURN-MARS I** code.³⁵ Note that the mixing of

TABLE VI. R factors obtained by considering α transfer to mixed configuration wave functions of ^{18}O states in the framework of Ref. 11.

Ex					
(MeV)	J_i^π	A_6^a	A_8^a	$R_{\text{MC}}^J \times 10^2{}^b$	$R_{\text{MC}}^J / R_{\text{MC}}^{0^+}{}^c$
g.s.	0_1^+	-0.2001	-0.1592	52.9	3.4 ± 1.9
1.98	2_1^+	-0.1723	-0.1859	14.0	0.9 ± 0.4
3.55	4_1^+	-0.1092	-0.0348	11.9	0.7 ± 0.3
3.63	0_2^+	0.0030	0.4405	15.8	1.0
3.92	2_2^+	0.0590	0.2685	17.3	1.1 ± 0.4
5.26	2_3^+	-0.1087	0.4249	25.5	1.6 ± 0.6
5.33	0_3^+	0.1275	-0.2604	23.7	1.5 ± 0.9
7.11	4_2^+	0.0563	0.4887	12.8	0.8 ± 0.3

^aThe $A_6^J = A_{2p}^J$ and $A_8^J = A_{4p-2h}^J$ are extracted from Ref. 11, but their phases are adjusted to the **SATURN-MARS I** code by the rule $A_Q^{SM} = (-)^N A_Q^{FK}$.

^bAs a in Table IV.

^cThe quoted errors come from statistical errors only.

TABLE VII. Comparison between the $R^J/R^{2_1^+}$ relative ratios of the present work and of the $^{14}\text{C}(^7\text{Li},t)^{18}\text{O}$ reaction analysis of Ref. 11.

Ex (MeV)	J_i^π	$R_{\text{MC}}^J/R_{\text{MC}}^{2_1^+}$ ^a	$(R_{\text{MC}}^J/R_{\text{MC}}^{2_1^+})_{\text{FK}}$ ^b	$R_8^J/R_8^{2_1^+}$ ^a	$(R_8^J/R_8^{2_1^+})_{\text{FK}}$ ^b
g.s.	0_1^+	3.8 ± 1.9	1.8	2.9 ± 0.5	2.3
1.98	2_1^+	1.0	1.0	1.0	1.0
3.55	4_1^+	0.8 ± 0.3	4.2	3.7 ± 0.6	3.0
3.63	0_2^+	1.1 ± 0.5		0.5 ± 0.1	
3.92	2_2^+	1.2 ± 0.4	1.2	0.6 ± 0.1	0.6
5.26	2_3^+	1.8 ± 0.5	1.6	0.43 ± 0.06	0.4
5.33	0_3^+	1.7 ± 0.9		0.33 ± 0.09	
7.11	4_2^+	0.9 ± 0.3	2.3	0.48 ± 0.06	1.0

^aThe quoted errors come from statistical errors only.

^bFrom the $^{14}\text{C}(^7\text{Li},t)^{18}\text{O}$ reaction at 20.4 MeV incident energy (Ref. 11).

the configurations does not change the shapes of the theoretical curves reported in Fig. 3 but only the absolute values.

In order to compare with data, we define ³³ an R -normalization factor by

$$\left(\frac{d\sigma}{d\Omega}\right)_{\text{exp}} = \left(\frac{d\sigma}{d\Omega}\right)_{\text{HF}} + R \left(\frac{d\sigma}{d\Omega}\right)_{\text{DWBA}}^{\text{MC}}. \quad (8)$$

If the A_{NL}^J are correctly evaluated, we expect constant R values for different transitions. Table VI summarizes the R values found, labeled as R_{MC}^J , and the relative ratios $R_{\text{MC}}^J/R_{\text{MC}}^{0_2^+}$. Good agreement to the unity is found, and, as shown in Table VII, consistency with the results of the similar analysis ¹¹ of the $^{14}\text{C}(^7\text{Li},t)^{18}\text{O}$ reaction is also found. The only exception is the g.s. R factor, which has the largest error bar.

Table VIII shows the results obtained by taking

into account *only* transfer to the main component, or to the 4p-2h component of the wave function, or by assuming a pure configuration. In this analysis the R factor values were evaluated from

$$R^J = \frac{S^J}{|\mathbf{a}_{2s} \cdot A_{NL}^J|^2}. \quad (9)$$

The comparison, shown in Fig. 7, evidentiates the crucial role played by the interference between α transfer to 2p and to 4p-2h components.

D. ^{18}O positive-rotational band

In this section we discuss our results in connection with the proposed ^{18}O rotational band ^{5,9,14} based on the 0^+ at 3.63 MeV. As is well known, ³⁶ a fairly good idea of rotational band membership can be obtained by looking to see if a series of states, all described in a similar way, fall on a

TABLE VIII. R factors evaluated by considering α transfer only to the main components ($R_{\text{main}}^J/R_8^{0_2^+}$) or only to the (4p-2h) components ($R_8^J/R_8^{0_2^+}$) or to “pure-configurations” ($R_{\text{PC}}/R_{\text{PC}}^{0_2^+}$) for low lying ^{18}O positive parity states. The quoted errors come from statistical errors only.

Ex (MeV)	J_i^π	$R_{\text{main}}^J/R_8^{0_2^+}$ ^a	$R_8^J/R_8^{0_2^+}$ ^a	$R_{\text{PC}}/R_{\text{PC}}^{0_2^+}$ ^b	Main configurations ^c
g.s.	0_1^+	5.9 ± 1.3	5.6 ± 1.2	14.8 ± 3.2	$(sd)^2$
1.98	2_1^+	20.5 ± 3.6	1.9 ± 0.3	94.1 ± 16.7	$(sd)^2$
3.55	4_1^+	14.5 ± 2.5	7.1 ± 1.3	40.2 ± 6.9	$(sd)^2$
3.63	0_2^+	1.0	1.0	1.0	$(sd)^4(p)^{-2}$
3.92	2_2^+	227.9 ± 36.6	1.2 ± 0.2	78.0 ± 12.5	$(sd)^2$
5.26	2_3^+	0.8 ± 0.1	0.8 ± 0.1	0.8 ± 0.1	$(sd)^4(p)^{-2}$
5.33	0_3^+	3.9 ± 1.2	0.6 ± 0.2	3.4 ± 1.1	$(sd)^2$
7.11	4_2^+	0.9 ± 0.1	0.9 ± 0.1	1.1 ± 0.2	$(sd)^4(p)^{-2}$

^aThe A_6^J and A_8^J values are those of Table VI.

^bThe A_6^J and A_8^J values are obtained, respectively, from Eqs. (6) and (7) putting C_{NL}^J or C_{NL}^J equal to unity. The configurations assumed as pure were the main ones.

^cFrom Refs. 4, 7, and 9.

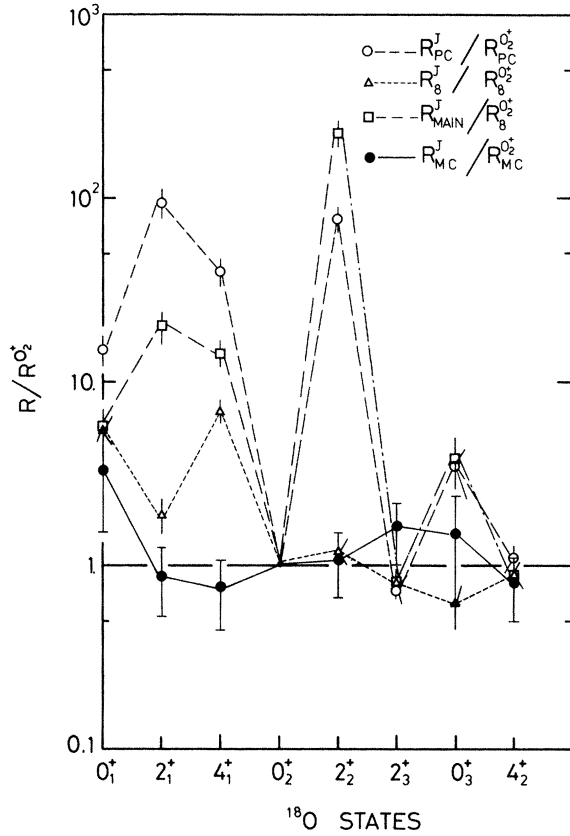


FIG. 7. Relative ratios $R/R_{0_2^+}$ for low-lying positive parity ^{18}O states. Squares refer to $R_{\text{MAIN}}^J/R_{0_2^+}^{0_2^+}$, triangles to $R_B^J/R_{0_2^+}^{0_2^+}$, open circles to $(R_{\text{PC}}^J/R_{0_2^+}^{0_2^+})$, and solid circles to $R_{\text{MC}}^J/R_{0_2^+}^{0_2^+}$ of the present work. (See text). The dashed curves are drawn to guide the eyes.

$J(J+1)$ curve and if they have similar θ_α^2 alpha reduced widths.

In Fig. 8 is shown a plot of excitation energy versus $J(J+1)$ values for the positive-parity ^{18}O states studied in the present work. The $J(J+1)$ criterion selects as possible candidates the 0_2^+ , 2_2^+ , 2_3^+ , 4_2^+ , 4_3^+ , 6_1^+ , and 6_2^+ states. Our results confirm the 4p-2h main character of the 3.63 MeV (0_2^+), 5.26 MeV (2_3^+), and 7.11 MeV (4_2^+) states as well as the 2p-0h one of the 3.92 MeV (2_2^+) state, i.e., the Lawson *et al.*⁴ predictions. For the levels at 7.84 MeV (4_3^+), 11.69 MeV (6_1^+), and 12.53 MeV (6_2^+) not treated in Ref. 4, we compare with the Sakuda⁷ predictions obtained mixing 2p shell-model states with α clustering of 4p-2h states. In effect we are not able to make a complete mixed-configuration calculation in these particular bases. However, looking at Fig. 7, one may note that the hypothesis of α transfer to 4p-2h configuration is, in our case, a rather good approximation. Therefore the experimental $S_8^J/S_8^{0_2^+}$

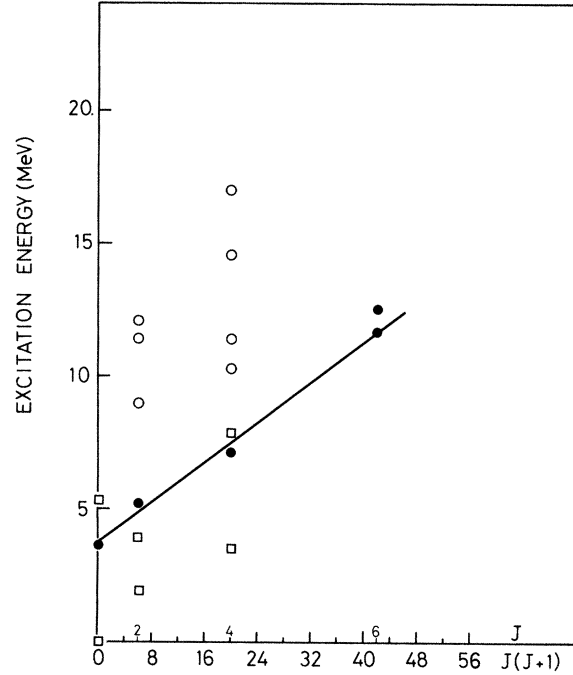


FIG. 8. Energies of the positive-parity ^{18}O states versus $J(J+1)$. Squares refer to (2p) main configuration states, solid circles to 4p-2h main configuration states, and open circles to states with no established configurations. The slope of the full line drawn gives $\hbar^2/2J_0 = 0.186$.

ratios are compared in Table IX with the $S_\alpha/S_\alpha^{0_2^+}$ values calculated taking into account complete mixing.⁷ The rather good overall agreement found corroborates the Sakuda predictions,⁷ i.e.,

- (i) the 4p-2h character of the 0_2^+ , 2_3^+ , and 4_2^+ states;
- (ii) the mixed structure of the 4_3^+ state with a slightly dominant 2p component (also inferred from the empirical analyses outlined in Secs. II and IV B;

TABLE IX. Comparison between experimental relative α -spectroscopic strengths $S_8^J/S_8^{0_2^+}$ and the Sakuda (Ref. 7) theoretical predictions.

E_x (MeV)	J_i^π	$S_8^J/S_8^{0_2^+}$ ^a	$(S_\alpha^J/S_\alpha^{0_2^+})_{\text{SAK}}$ ^b	Suggested main configurations ^b
3.63	0_2^+	1.0	1.0	"4p-2h"
5.26	2_3^+	0.8 ± 0.1	1.3	"4p-2h"
7.11	4_2^+	1.1 ± 0.2	1.0	"4p-2h"
7.84	4_3^+	0.3 ± 0.1	0.5	2p-0h
11.69	6_1^+	0.9 ± 0.2	1.1	"4p-2h"
12.53	6_2^+	0.42 ± 0.06	0.3	"4p-2h"

^aThe quoted errors come from statistical errors only.

^bFrom Ref. 7. The quotation marks indicate particular collective states (see text).

(iii) the collective nature of both the 11.69 MeV(6_1^+) and the 12.53 MeV(6_2^+) states. Moreover the smallness of the 6_2^+ relative α -spectroscopic strength is consistent with the main core excited structure suggested⁷ for this state.

On the other hand, the relative α -spectroscopic strengths $S_8^J/S_8^{0_2^+}$, in Table IX, are about the same for 0_2^+ , 2_3^+ , 4_2^+ , and 6_1^+ states.

All these results allow us to support the suggestions that the 2_3^+ at 5.26 MeV, the 4_2^+ at 7.11 MeV, and the 6_1^+ at 11.69 MeV are the members of the ^{18}O rotational band based on the 3.63 MeV(0_2^+) level. Finally we remark that for the proposed ^{18}O rotational band a linear best fit gives $\hbar^2/2J_0 = 0.186 \pm 0.012$, which essentially agrees with the value 0.146 calculated by Rudra¹⁴ by means of a cranking model, as well as with the slope of the g.s. rotational band in ^{20}Ne , as proposed in Ref. 9.

IV. CONCLUSIONS

The shape of the experimental angular distributions and the smallness of the statistical compound nucleus contribution indicate that the $^{14}\text{C}(^6\text{Li}, d)^{18}\text{O}$ at 34 MeV incident energy proceeds essentially via an α -transfer direct mechanism.

The analysis of data leads us to suggest 4^+ spin and parity to the 7.84 MeV level and 2^+ to the 8.9 and 12.04 MeV levels and, to some extent, 4^+ for the 14.6 and 17.0 MeV levels.

The analysis of α -spectroscopic strengths confirms the theoretical predictions^{4,7,9} about configuration mixing, as well as the importance of the interference between α transfer to two particles and 4p-2h collective components of the ^{18}O states. A very good agreement is found using the empirical wave functions of Ref. 4.

The results found in (i) the configurations analysis, (ii) the plot of the excitation energy versus $J(J+1)$, and (iii) the comparison of the relative α -spectroscopic strengths, confirm the predicted^{5,9} ^{18}O positive rotational band based on the first excited 0_2^+ at 3.63 MeV (being the 5.26 MeV 2_3^+ , the 7.11 MeV 4_2^+ , and the 11.69 MeV 6_1^+ the other members). ($^6\text{Li}, d\alpha$) angular correlation measurements are in progress in order to check the spins and parities currently suggested and to determine $\Gamma_\alpha/\Gamma_{\text{tot}}$ values³⁷ for ^{18}O levels lying at excitation energies above the α -emission threshold.

The authors would like to thank Dr. N. Mascolo for her help in experimental data processing.

-
- ¹F. Ajzenberg-Selove, Nucl. Phys. **A300**, 1 (1978).
²T. Engeland, Nucl. Phys. **72**, 68 (1965).
³H. T. Fortune and S. C. Headley, Phys. Lett. **51B**, 136 (1974).
⁴R. D. Lawson, F. J. D. Serduke, and H. T. Fortune, Phys. Rev. C **14**, 1245 (1976).
⁵B. Buck, H. Friedrich, and A. A. Pilt, Nucl. Phys. **A290**, 205 (1977).
⁶M. Lemere, Y. C. Tang, and D. R. Thompson, Phys. Rev. C **16**, 475 (1977).
⁷T. Sakuda, Prog. Theor. Phys. **57**, 855 (1977).
⁸T. Sakuda, S. Nagata, and F. Nemoto, Prog. Theor. Phys. **59**, 1543 (1978).
⁹T. Erikson and G. E. Brown, Nucl. Phys. **A277**, 1 (1977).
¹⁰B. Buck and A. A. Pilt, Nucl. Phys. **A295**, 1 (1978).
¹¹H. T. Fortune and D. Kurath, Phys. Rev. C **18**, 236 (1978).
¹²J. L. Wiza, R. Middleton, and P. V. Hewka, Phys. Rev. **141**, 975 (1966); T. K. Li, D. Dehnard, R. E. Brown, and P. J. Ellis, Phys. Rev. C **13**, 55 (1976); J. C. Armstrong and K. S. Quisenberry, Phys. Rev. **122**, 150 (1961).
¹³R. Middleton and D. J. Pullen, Nucl. Phys. **51**, 63 (1964).
¹⁴N. Rudra, Nucl. Phys. **A312**, 33 (1978).
¹⁵G. L. Morgan, D. R. Tilley, G. E. Mitchell, R. A. Hilko, and N. R. Roberson, Phys. Lett. **32B**, 353 (1970).
¹⁶A. A. Ogloblin, in *Proceedings of the Fifth International Conference on Nuclear Reactions Induced by Heavy Ions, Heidelberg, Germany, 1969*, edited by R. Bock and W. R. Hering (North-Holland, Amsterdam, 1970); see also reviews given by K. Bethge, Annu. Rev. Nucl. Sci. **20**, 225 (1970).
¹⁷A. Cunsolo, A. Foti, G. Immè, G. Pappalardo, G. Raciti, and N. Saunier, Report No. CEA-N-2070, 1977/78, p. 31; A. Cunsolo, A. Foti, G. Immè, G. Pappalardo, G. Raciti, F. Rizzo, and N. Saunier, in *Proceedings of the 2nd International Conference on Nuclear Reaction Mechanism, Varenna, Italy, 1979* (Clued, Milano, 1979), p. 363.
¹⁸L. Bianchi and P. Bouyer, Report No. CEA-N-1522, 1970/71, p. 93.
¹⁹J. B. A. England, R. Bhowmik, F. D. Brooks, E. C. Pollacco, N. E. Sanderson, and G. C. Morrison, *Lecture Notes in Physics* (Springer, New York, 1979), Vol. 92, p. 470.
²⁰S. J. Sanders, L. M. Martz and P. D. Parker, in *Proceedings of the International Conference on Nuclear Structure, Tokyo, 1977*, p. 177; L. M. Martz, thesis, Yale University, 1978 (unpublished).
²¹G. L. Morgan, D. R. Tilley, G. E. Mitchell, R. A. Hilko, and N. R. Roberson, Nucl. Phys. **A148**, 480 (1970).
²²A. Cunsolo, A. Foti, G. Pappalardo, G. Raciti, and N. Saunier, Phys. Rev. C **18**, 856 (1978) and references therein.
²³W. Hauser and H. Feshbach, Phys. Rev. **87**, 366 (1952); H. Feshbach, in *Nuclear Spectroscopy*, edited by F. Aj-

- zenberg-Selove (Academic, New York, 1960).
- ²⁴K. Bethge, D. J. Pullen, and R. Middleton, *Phys. Rev. C* **2**, 395 (1970).
- ²⁵A. Cunsolo, A. Foti, G. Immè, G. Pappalardo, G. Raciti, N. Saunier, and B. T. Kim, *Nucl. Phys.* **A355**, 261 (1981).
- ²⁶T. Tamura and K. S. Low, *Comput. Phys. Commun.* **8**, 349 (1974).
- ²⁷R. M. De Vries, H. W. Fulbright, R. G. Markham, and U. Strohmusch, *Phys. Lett.* **55B**, 33 (1975).
- ²⁸U. Strohmusch, G. Bauer, and H. W. Fulbright, *Phys. Rev. Lett.* **34**, 968 (1975).
- ²⁹N. Anantaraman, H. E. Gove, J. P. Trentelman, J. P. Draayer, and F. C. Jundt, *Nucl. Phys.* **A276**, 119 (1977).
- ³⁰G. D. Gunn, R. N. Boyd, N. Anantaraman, D. Shapira, J. Töke, and H. E. Gove, *Nucl. Phys.* **A275**, 524 (1977).
- ³¹H. W. Fulbright, C. L. Bennett, R. A. Lindgreen, R. G. Markham, S. C. Mc Guire, G. C. Morrison, U. Strohmusch, and J. Töke, *Nucl. Phys.* **A284**, 329 (1977).
- ³²N. Anantaraman, H. E. Gove, R. A. Lindgreen, J. Töke, J. P. Trentelman, J. P. Draayer, F. C. Jundt, and G. Guillaume, *Nucl. Phys.* **A313**, 445 (1979).
- ³³A. Cunsolo, A. Foti, G. Immè, G. Pappalardo, G. Raciti, and N. Saunier, *Lett. Nuovo Cimento* **23**, 371 (1978).
- ³⁴N. Austern, *Direct Nuclear Reaction Theories* (Wiley, New York, 1970); T. Tamura, *Phys. Rep.* **14**, 59 (1974).
- ³⁵J. C. Peng, private communication.
- ³⁶A. A. Pilt and H. T. Fortune, *Lett. Nuovo Cimento* **21**, 502 (1978).
- ³⁷A. Cunsolo, A. Foti, G. Immè, G. Pappalardo, G. Raciti, and N. Saunier, *Phys. Rev. C* **21**, 2345 (1980).
- ³⁸D. Wilmore and P. E. Hodgson, *Nucl. Phys.* **55**, 673 (1964).
- ³⁹F. G. Perey, *Phys. Rev.* **131**, 745 (1963).
- ⁴⁰E. Newman, L. C. Becker, B. M. Freedom, and J. C. Hiebert, *Nucl. Phys.* **A100**, 225 (1967).
- ⁴¹R. N. Glover and A. D. W. Jones, *Nucl. Phys.* **81**, 268 (1966).
- ⁴²W. Bohne, H. Homeyer, H. Lettau, H. Morgenstern, J. Scheer, and F. Sichelschmidt, *Nucl. Phys.* **A160**, 257 (1971).